

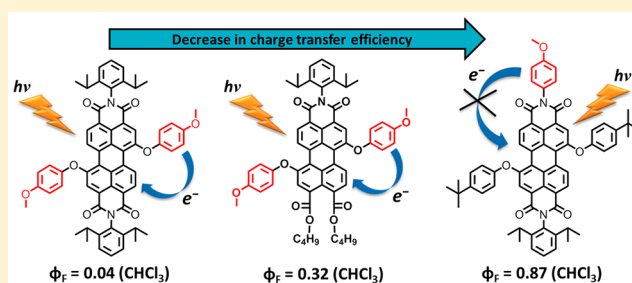
Substitution Effects on the Photoinduced Charge-Transfer Properties of Novel Perylene-3,4,9,10-tetracarboxylic Acid Derivatives

Damla Inan,[†] Rajeev K. Dubey,^{†,‡} Nick Westerveld,[‡] Jorrit Bleeker,[†] Wolter F. Jager,^{*,‡} and Ferdinand C. Grozema^{*,†}

[†]Laboratory of Optoelectronic Materials and [‡]Laboratory of Organic Materials & Interfaces Department of Chemical Engineering, Delft University of Technology, Van der Maasweg 9, 2629 HZ Delft, The Netherlands

Supporting Information

ABSTRACT: We report here the synthesis and photophysical study of a series of electron donor–acceptor molecules, in which electron-donating 4-methoxyphenoxy groups are attached to the 1,7-bay positions of four different perylene tetracarboxylic acid derivatives, namely, perylene tetraesters **1**, perylene monoimide diesters **2**, perylene bisimides **3**, and perylene monobenzimidazole monoimides **4**. These perylene derivatives are used because of their increasing order of electron-accepting capability upon moving from **1** to **4**. Two additional donor–acceptor molecules are synthesized by linking electron-donating 4-methoxyphenyl groups to the imide position of perylene monoimide diester **2** and perylene bisimide **3**. The motivation for this study is to achieve a good control over the photoinduced charge-transfer (CT) process in perylene-based systems by altering the position of electron donors and tuning the electron deficiency of perylene core. A comprehensive study of the photophysical properties of these molecules has shown a highly systematic trend in the magnitude of CT as a function of increased electron deficiency of the perylene core and solvent polarity. Importantly, just by changing the attachment of electron-donating group from “bay” to “imide” position, we are able to block the CT process. This implies that the positioning of the electron donor at the perylene core strongly influences the kinetics of the photoinduced CT process. In these compounds, the CT process is characterized by the quenching of fluorescence and singlet excited-state lifetimes as compared to model compounds bearing non-electron-donating 4-*tert*-butylphenoxy groups. Transient absorption spectroscopy did not reveal spectra of CT states. This most likely implies that the CT state is not accumulated, because of the faster charge recombination.



INTRODUCTION

A good control over photoinduced charge and energy transfer between donor and acceptor moieties is essential for the development of artificial photosynthesis.^{1–4} Important variables, which dictate the yields and kinetics of these interactions, are excited-state and redox properties of the donor and acceptor components, their relative distance, mutual orientation, and electronic coupling.^{5–10} During the past three decades, molecular assemblies consisting of light-harvesting chromophores, charge separators, and catalysts have been designed and studied to gain a better understanding of the photochemistry and photophysics involved in these systems.^{11–13} Such assemblies are of prime importance because of their ability to mimic the natural photosynthetic process and to convert sunlight into fuel.

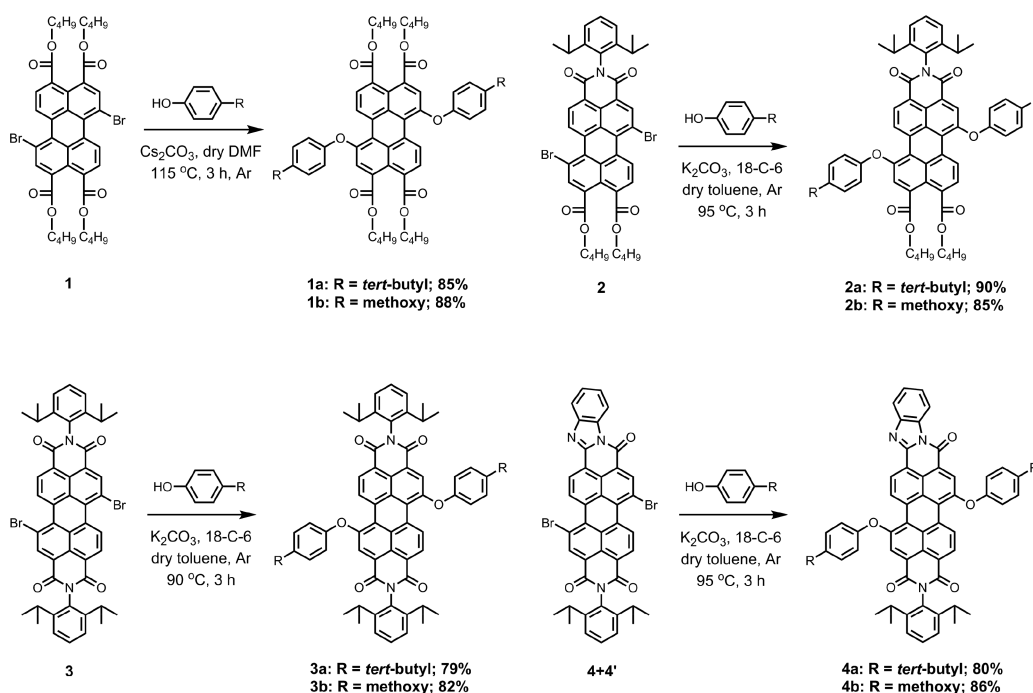
Several chromophores have been tested as integrative building blocks for light-harvesting and charge separation. Perylene tetracarboxylic acid derivatives, of which perylene bisimides (PBIs) are the best-known representatives, are particularly attractive chromophores due to their exceptional photochemical stability, high electron deficiency, strong absorption in the visible region of the solar spectrum, and

possibility to further tune their photophysical properties by structural modifications.^{14,15} Taking advantage of high photochemical robustness and strong absorption, various light-harvesting antenna systems have been prepared using perylene tetracarboxylic acid derivatives as the active chromophore.^{16–18,10} However, because of the high electron deficiency of the perylene core, charge separation has been commonly observed when these compounds are covalently coupled even with moderately electron-rich donors.^{18,19}

Perylene tetracarboxylic acid derivatives (mostly PBIs) are also attractive components of charge separators, and for this application, their high electron deficiency is highly beneficial. In the past, many separate studies on perylene-based donor–acceptor systems have been performed.^{19–23} These studies have revealed that the efficiency and kinetics of charge transfer (CT) are highly sensitive to even small structural variations. In a recent study on PBI-based isoelectronic donor-bridge-acceptor compounds, we showed that small changes in the molecular bridge have a large impact on the dynamics of charge

Received: April 23, 2017

Published: May 30, 2017

Scheme 1. Synthesis of 1,7-Di(4-*tert*-butylphenoxy) and 1,7-Di(4-methoxyphenoxy)perylene-3,4,9,10-tetracarboxylic Acid Derivatives

separation.²⁴ In another recent study, Shoer et al. observed that the charge separation can be an order of magnitude faster for systems in which donors are connected to the ortho (or headland) positions of the perylene core as compared to the imide position.²⁵

Another recent study by Pagoaga et al. reported strong fluorescence quenching ascribed to charge separation, for PBIs bearing 4-methoxybenzene substituents as electron donors at various bay positions.²⁶ Preceding work by Flamigni et al. on non-bay-substituted PBIs, bearing mono-, di-, and trimethoxybenzene at the imide position, has revealed that CT rates strongly correlate with the redox properties of the methoxybenzene and the positioning of the methoxy group.²⁷ A comparison between efficiency of CT and the positioning of the electron donors cannot be made from these studies, because 1,7-bay substitution decreases the reduction potential of the perylene acceptor, that is, makes the perylene core less electron-deficient.¹⁴ Therefore, there is still a need for a comprehensive study to understand the kinetics of CT toward perylenes as a function of the position at which the electron-donating substituents are attached, so that perylene-containing devices can be designed in which the perylene derivatives serve a well-defined role of energy acceptor or donor in a light harvesting antenna and that of electron acceptor in a charge-separating unit.

In this work, we report on the design, the synthesis, and the photophysical properties of a series of perylene-3,4,9,10-tetracarboxylic acid derivatives bearing either 4-methoxyphenoxy or 4-methoxyphenyl groups as electron donors. The choice of these groups as electron donors is based on reports in which facile CT was observed upon photoexcitation of perylene bisimides bearing methoxyphenyl groups as electron donors.^{26,27} In this study, the electrochemical and optical properties of the perylene core were also systematically tuned by the modifications at the peri-positions. For the photophysical characterization of our compounds, steady-state and

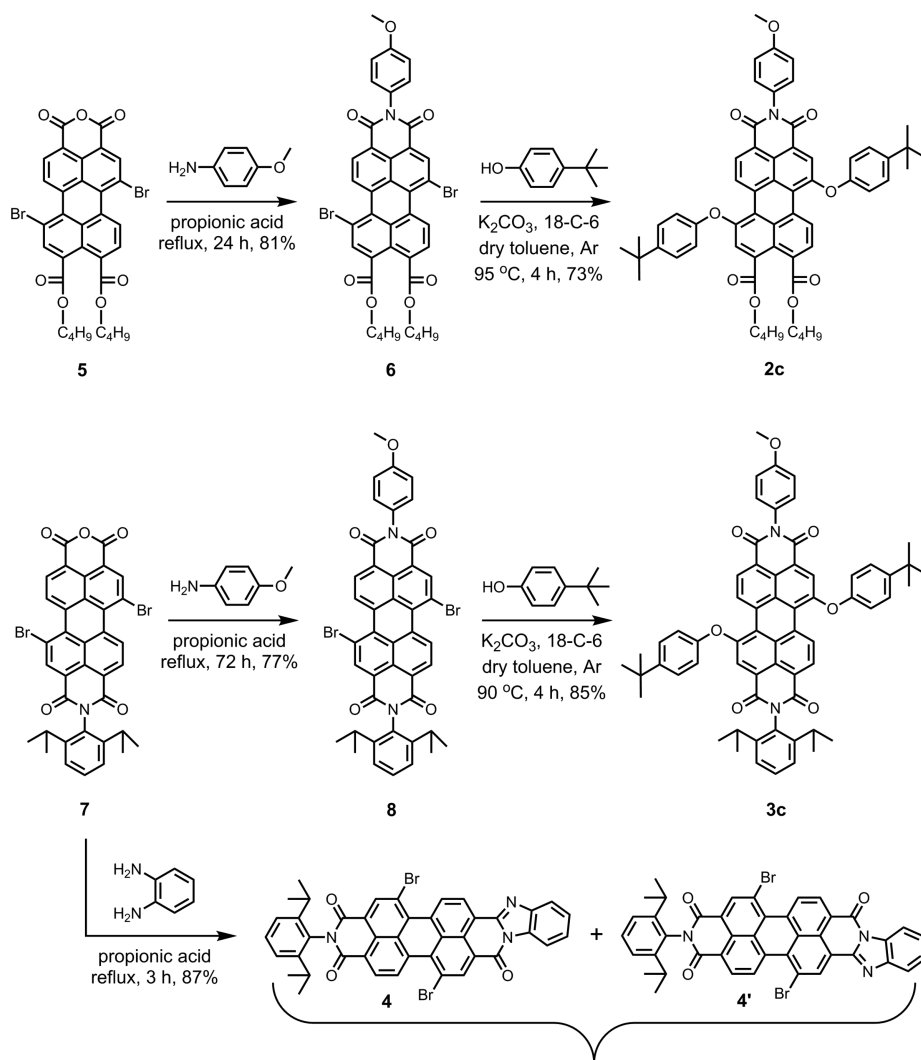
time-resolved spectroscopic studies were performed in solvents of different polarity. In these compounds, the strong fluorescence of the perylene moiety was quenched to different extent by electron-donating groups attached to the perylene core at different positions. The aim of this work is to establish a relation between molecular structure and the extent of fluorescence quenching observed for these molecules in solvents of different polarity. We ascribe this fluorescence quenching to photoinduced CT and assume that the positions from which quenching is efficient are the appropriate positions to attach electron donors and achieve efficient charge separation. Finally, the obtained experimental results are rationalized by computational calculations based on time-dependent density functional theory (TD-DFT).

RESULTS AND DISCUSSION

Synthesis and Characterization. As described in Scheme 1, the reported 1,7-diphenoxyperylene-3,4,9,10-tetracarboxylic acid derivatives (1a–b, 2a–c, 3a–c, and 4a–b) were synthesized from their corresponding 1,7-dibromoperylene-3,4,9,10-tetracarboxylic acid derivatives, 1,7-dibromoperylene tetrabutylester **1**, *N*-(2,6-diisopropylphenyl)-1,7-dibromoperylene monoimide dibutylester **2**, *N,N'*-bis(2,6-diisopropylphenyl)-1,7-dibromoperylene bisimide **3**, and the *N*-(2,6-diisopropylphenyl)-1,7-dibromoperylene monoimide monobenzimidazoles (**4** and **4'**).

The syntheses of these regioisomerically pure 1,7-dibromoprecursors (**1–4**) was performed from commercially available perylene-3,4,9,10-tetracarboxylic bisanhydride (PBA) using a previously reported procedure.²⁸ The subsequent substitution of bromine atoms with 4-*tert*-butylphenoxy and 4-methoxyphenoxy groups was achieved in high yields (80–90%) as shown in Scheme 1. The phenoxy substitution on 1,7-dibromoperylene tetrabutylester **1** was performed in anhydrous dimethylformamide (DMF) at elevated temperature (115 °C) owing to the low reactivity of the 1,7-dibromoperylene tetrabutylester toward nucleophilic substitution reactions.²⁸

Scheme 2. Synthesis of 4-Methoxyphenyl Functionalized Derivatives 2c and 3c



For all other derivatives (2, 3, and 4), the reaction was performed under milder reaction conditions in toluene at temperatures ~ 90 °C.^{10,29}

An isomeric mixture of 1,7-dibromoperylene monoimide monobenzimidazole compounds (4 + 4') was obtained by the reaction between 1,7-dibromoperylene monoimide monoanhydride 7 and 1,2-diaminobenzene in refluxing propionic acid (Scheme 2).³⁰ The thin-layer chromatography (TLC) analysis of this mixture revealed two slightly separated spots corresponding to 4 and 4'. Efforts to separate the two regioisomers by column chromatography, however, were not successful. The presence of two isomers was also evident from the ^1H NMR spectrum, in which two sets of signals in the aromatic region are clearly visible (Figure 1). These signals, corresponding to the perylene core protons H^8 , $\text{H}^{8'}$ and H^{11} , $\text{H}^{11'}$, were very well-resolved. On the basis of the relative intensities of these signals, surprisingly, the two regioisomers (4 and 4') were found in a ratio of ca. 2:1. The obtained ratio is rather surprising, because we cannot deduct differences in electron density of both anhydride carbonyl in compound 7, based on resonance structures. Thus, the reactivity of both anhydride carbonyl moieties is expected to be identical. For the synthesis of tetrachlorobisimidazoles, both 1:1³¹ and 2:1³² isomeric mixtures have been reported. The assignment of the

signals (H^8 , $\text{H}^{8'}$ and H^{11} , $\text{H}^{11'}$) to the individual regioisomers was done based on ^1H - ^1H COSY, and by the direct comparison of ^1H NMR spectrum of (4 + 4') with the spectrum of 1,7-dibromoperylene bisimide 3 (Figure 1). The ring current effect of the additional aromatic benzimidazole moiety was a decisive argument for explaining changes in the chemical shifts.

When comparing the ^1H NMR spectra of compounds 3 and 4 + 4', the chemical shifts for the perylene core protons H^2 and H^5 , in the "left" imide part of these compounds, are expected to be very similar. Indeed, protons H^2 and H^5 have identical chemical shifts in compounds 3 and 4 + 4'. Placement of the imidazole moiety on the "right" part of the molecule should effect the chemical shifts of protons H^8 and H^{11} , upon going from 3 to 4 or 4', but to a different extent. A larger shift is expected for the proton H^{11} in compound 4, whereas the imidazole placement in compound 4' should have a larger effect on the chemical shift of proton $\text{H}^{8'}$. The predicted shifts are clearly visible in the ^1H NMR spectrum depicted in Figure 1, in which the proton assignment is shown.

The two compounds 2c and 3c, containing 4-methoxyphenyl moiety at the imide position, were synthesized to investigate photoinduced CT from substituents attached to the imide position of perylene tetracarboxylic acid derivatives 2 and 3.

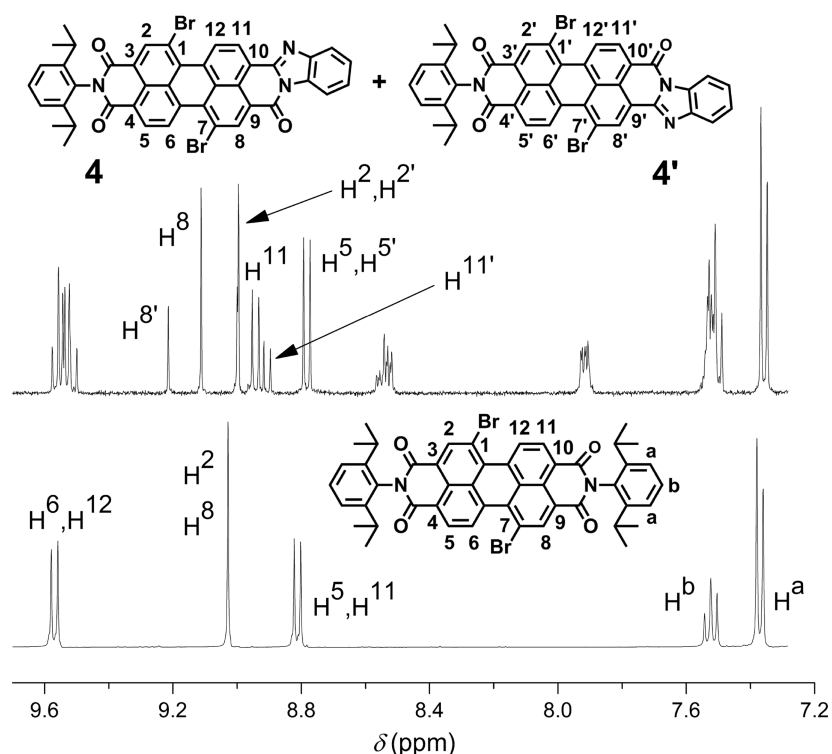


Figure 1. Comparison between ^1H NMR spectra of compound **4** + **4'** and 1,7-dibromoperylene bisimide **3**.

The synthesis was performed in two steps from their corresponding mono-anhydride precursors **5** and **7**, respectively. In the first step, imidization was performed with 4-methoxyaniline in refluxing propionic acid to afford corresponding imides **6** and **8**.²⁹ Thereafter, nucleophilic substitution of bromine atoms with 4-*tert*-butylphenol yielded the desired products **2c** and **3c** in good yields.

Electrochemical Studies. The redox properties of compounds **1–4** were investigated by cyclic voltammetry in dichloromethane. The obtained redox potentials (V vs Fc/Fc⁺) for these molecules are summarized in Table 1.

As shown in Table 1, the redox properties of the molecules change significantly if the substitution at the peri-positions is altered. When the groups attached to peri positions become more electron-withdrawing (e.g., from tetraester to mono-imide), the redox potentials of the compounds become more positive.^{32,33} This clearly shows that molecules have higher

electron affinities going from compound **1** to **2** to **3**, which makes them better electron acceptors. From the data in Table 1, it is clearly seen that the perylene tetracarboxylic derivatives **3** and **4** are rather similar as far as their electronic properties are concerned. This implies that the imide and benzimidazole groups are electrochemically equivalent.³² Finally, it is apparent that attaching different phenoxy groups at the bay positions does not result in notably different redox potentials. This indicates the absence of significant interaction between these groups in the ground state.

Steady-State Absorption Studies. The absorption spectra of compounds **1–4**, in chloroform, are shown in Figure 2, and the relevant data, in toluene, chloroform, and acetonitrile (or benzonitrile), are given in Table 2. All compounds are readily soluble in toluene and chloroform. However, the solubility in polar and weakly polarizable acetonitrile was much lower. Especially, the compounds **4a** and **4b** were insoluble in this solvent. At low solubility, perylene derivatives tend to aggregate.³⁴ This aggregation alters the optical properties and optoelectronic performances. In general, spectral broadening and shifts in absorption and emission spectra, along with fluorescence quenching, are the common signatures of this aggregation.^{35,36} Therefore, to preclude spectral changes caused by aggregation, benzonitrile was used as a polar solvent for compounds **3** and **4**.

The absorption spectra of all donor-substituted compounds (**1b–4b**) are characterized by a strong absorption band at longer wavelengths (425–625 nm) and a weaker absorption band at shorter wavelengths (Figure 2). As shown previously in literature, bay substitution leads to a disappearance of the pronounced vibronic structure observed for perylenes without bay substitution. This is accompanied by a bathochromic shift of the absorption bands.^{29,37} When the size of the π -system increased, that is, going from compounds **1** to **2** to **3** and **4**, the molar extinction coefficient increases gradually, and the

Table 1. First Redox Potentials of Perylene Derivatives (V vs Fc/Fc⁺) Obtained by Cyclic Voltammetry in CH₂Cl₂

compound	$E_{1/2 \text{ ox}}$	$E_{1/2 \text{ red}}$
1		−1.55
1a	+0.84	<i>a</i>
1b	+0.82	<i>a</i>
2a	+0.95	−1.38 ^b
2b	+0.94	−1.38
2c	+0.97	−1.33
3a	+1.05	−1.11
3b	+1.04	−1.10
3c	+1.06	−1.09
4a	+1.01	−1.06
4b	+1.02	<i>c</i>

^aNo reduction potential was observed. ^bIrreversible. ^cNot detectable.

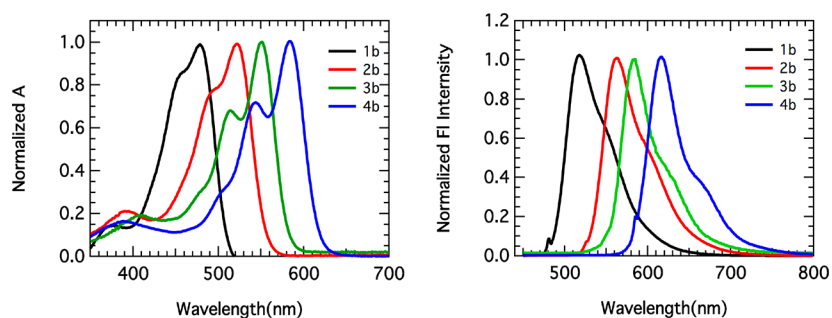


Figure 2. Normalized UV/vis absorption (left) and emission spectra (right) of the compounds 1–4b in chloroform.

Table 2. Optical Properties of Compounds in Toluene, Chloroform, Acetonitrile/Benzonitrile

compound	solvent	λ_{abs} (nm)	λ_{em} (nm)	ϵ ($\text{M}^{-1} \text{cm}^{-1}$)	$\Phi_{\text{F}}^{\text{a}}$	τ_{F} (ns) ^b
1a	toluene	475	515	31 500	0.91	4.26
	chloroform	475	515	25 600	0.84	4.40
	acetonitrile	471	512	24 800	0.90	4.73
1b	toluene	479	515	24 000	0.88	4.25
	chloroform	478	517	29 300	0.81	4.38
	acetonitrile	479	517	33 200	0.02	~0.21 ^c
2a	toluene	515	552	38 900	0.85	4.52
	chloroform	517	557	36 700	0.87	4.82
	acetonitrile	512	563	31 700	0.90	5.23
2b	toluene	520	555	34 300	0.85	4.34
	chloroform	522	561	36 000	0.32	3.21
	acetonitrile	517	566	34 100	0.03	~0.08 ^c
2c	toluene	513	549	35 900	0.93	4.36
	chloroform	519	563	36 900	0.87	4.73
	acetonitrile	511	558	34 700	0.92	4.69
3a	toluene	543	572	57 800	0.94	4.44
	chloroform	547	578	54 200	0.91	4.64
	benzonitrile	552	586	54 600	0.86	4.47
3b	toluene	549	575	53 300	0.19	~0.71 ^c
	chloroform	551	580	53 100	0.04	~0.43 ^c
	benzonitrile	561	583	51 400	0.01	~0.12 ^c
3c	toluene	542	572	52 500	1.00	3.80
	chloroform	548	577	51 000	0.87	3.89
	benzonitrile	555	582	50 900	0.63	3.30
4a	toluene	578	607	63 600	0.71	4.42
	chloroform	581	614	63 700	0.66	4.31
	benzonitrile	584	619	61 350	0.70	4.22
4b	toluene	582	609	63 300	0.75	4.22
	chloroform	584	616	67 600	0.23	2.45
	benzonitrile	591	621	69 500	0.04	~0.43 ^c

^aFluorescence quantum yield. ^bFluorescence lifetime. ^cNon-monoexponential decay.

absorption maxima shift to longer wavelengths. When the bay substituent attached to the perylene core is changed from *tert*-butylphenoxy to 4-methoxyphenoxy is changed, small 5 nm red shifts are observed. The influence of solvent polarity on the absorption maxima is rather modest. Positive solvatochromism, a red shift in absorption upon increasing the solvent polarity, was observed, in particular, for compounds with more electron-deficient perylene cores, but these spectral shifts do not exceed 15 nm.

Steady-State and Time-Resolved Emission Studies.

The emission spectra of compounds 1–4 roughly resemble the mirror images of the corresponding absorption spectra (Figure 2). The positions of the emission wavelengths exhibit the same trend as those of the absorption maxima (Table 2). While the effects of changing the bay substituents and solvent polarity on

the emission wavelengths of these perylene compounds are modest, the emission intensities, quantified by their fluorescence quantum yields (Φ_{F}), are extremely sensitive to these parameters. Fluorescence quantum yields close to unity with fluorescence lifetimes (τ_{F}) in the 4–5 ns range are observed for compounds bearing the non-electron-donating *tert*-butylphenoxy substituents at the bay positions (compounds 1a–4a, Table 2).²⁹ These fluorescent properties are similar to those of non-bay-substituted perylenes; that is, no significant fluorescence quenching occurs from the 4-*tert*-butylphenoxy substituents. Note that the high fluorescence of compound 4a in toluene is remarkable, because fluorescence quantum yields of perylene benzimidazoles are, in general, substantially lower as compared to perylene bisimides.³²

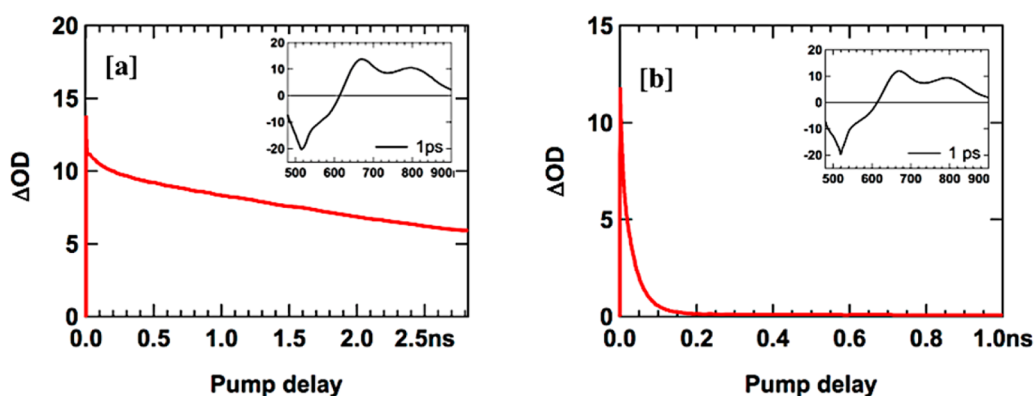


Figure 3. Kinetic traces at photoinduced absorption (685 nm) of molecules **2a** [a] and **2b** [b] in acetonitrile. The transient absorption spectrum immediately after excitation (inset).

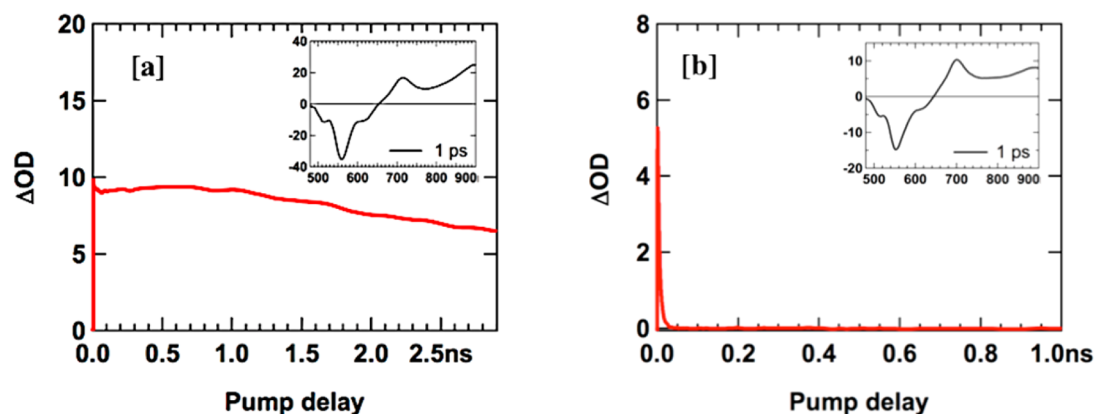


Figure 4. Kinetic traces at photoinduced absorption (775 nm) of molecules **3a** [a] and **3b** [b] in benzonitrile. The transient absorption spectrum immediately after excitation (inset).

For the compounds bearing the electron-donating 4-methoxyphenoxy substituents at the bay positions (compounds **1b–4b**), fluorescence quantum yields gradually decreased with the increase in solvent polarity and electron deficiency of the perylene core. The effect of solvent polarity is clearly illustrated by compound **2b** that has strong fluorescence in toluene ($\Phi_F = 0.75$) but shows negligible fluorescence in acetonitrile ($\Phi_F = 0.03$). The effect of the increased electron deficiency of the perylene core is clearly illustrated by the weak fluorescence found for compound **3b** in all solvents. These observations suggest that quenching of perylene fluorescence in these compounds is induced by photoinduced CT, although other quenching mechanisms cannot be excluded.³⁸

To establish whether the quenching depends on the position at which the electron-donating substituent is attached to the perylene core, the optical properties of the bay-substituted compounds **2b** and **3b** are compared to the corresponding imide-substituted compounds **2c** and **3c**. The fluorescence of the bay-substituted compounds **2b** and **3b** is much weaker compared to the compounds **2c** and **3c**. This is clearly seen by comparing the fluorescence of compound **2b** with that of compound **2c**. While the fluorescence of **2b** strongly decreases upon increasing the solvent polarity, compound **2c** remains strongly fluorescent in all solvents. A similar observation is made by comparing the fluorescence of compounds **3b** and **3c**. Note that ascribing the differences in photophysical properties between **2b** and **2c**, and **3b** and **3c** solely to the positioning of the electron donor is not entirely valid. This is mainly because the number of electron-donating substituents is different in

both cases, and the oxidation potential of the 4-methoxyphenoxy bay substituent is ca. 0.30 V lower than that of the methoxyphenyl imide substituent.³⁹ However, since it has been previously shown that 4-methoxyphenyl substituents at all bay positions strongly quench the fluorescence of PBIs,²⁶ it can still be concluded that fluorescence quenching from bay position is substantially faster than from imide position. This conclusion is further supported by a previous report,⁴⁰ in which we observed that the fluorescence quenching of perylene tetraester by an aniline electron donor is substantially faster from the bay position as compared to the peri-position.

Time-resolved fluorescence spectroscopy reveals that the fluorescence of the strongly emitting compounds ($\Phi_F > 0.2$) decays monoexponentially. Additionally, the emission of these compounds is not significantly influenced by the presence of oxygen. Using the fluorescence quantum yields and the fluorescence lifetimes, the rates of fluorescence and of nonradiative decay (quenching by CT) were calculated and summarized in Table S1 (Supporting Information). From this table it is evident that upon increasing the solvent polarity, lifetimes and rates of fluorescence decrease for all compounds. Rates of fluorescence between 2.5 and $1 \times 10^8 \text{ s}^{-1}$ were determined for all compounds, and these rates do not appear to be influenced by the bay substituents. Quenching rates are in the order of $1 \times 10^7 \text{ s}^{-1}$ for the nonquenched compounds. For the strongly quenched compounds, rates of quenching (and fluorescence) cannot be determined accurately, because fluorescence decay is no longer monoexponential. Nevertheless,

CT rates are estimated to be in the order from 1×10^9 to $1 \times 10^{10} \text{ s}^{-1}$.

Transient Absorption Spectroscopy. To investigate the time-resolved photophysics in more detail, we selected two series of compounds (**2a–c** and **3a–c**) for which femtosecond pump–probe transient absorption spectroscopy measurements were performed. In these series, the molecules have different substitution patterns, nearly identical absorption spectra, and markedly different rates of fluorescence quenching in polar solvents. The transient absorption spectra were measured in either acetonitrile (**2a–2c**) or benzonitrile (**3a–3c**) using pump wavelengths between 510 and 550 nm. The transient absorption spectra for compounds **2a** and **2b**, and **3a** and **3b**, immediately after excitation are shown in the inset in Figures 3 and 4, respectively. These transient spectra are very similar to previously reported spectra with pronounced excited-state absorption features.^{10,19,24,41} For the monoimide compounds (**2a,b,c**) ground-state bleaching below 520 nm, stimulated emission between 520 and 620 nm, and a broad excited-state absorption with two maxima near 685 and 800 nm are observed. For the bisimide compounds (**3a,b,c**) similar induced emission and absorption features are observed, but now the excited-state absorptions are shifted to longer wavelengths (710 and >900 nm). The spectra of **2c** and **3c** are depicted in Figure S5 in the Supporting Information. It is interesting that the spectra for compounds **2a** and **2b** and those of **3a** and **3b** are indistinguishable, even though very large differences in the radiative lifetime and fluorescence quantum yields were observed.

The identical photoinduced absorption spectra immediately after excitation (at 1 ps) indicate that the nature of the excited states is the same in both cases. However, the lifetimes of the excited states are much shorter for **2b** and **3b** than they are for **2a** and **3a**, respectively. To determine the lifetime of the singlet excited state of **2a–2c** and **3a–3c** we performed a global analysis. When we compared the lifetime of the singlet excited state with the fluorescence lifetime for all compounds in polar solvent, we see that these lifetimes are very close to the fluorescence lifetimes for all the compounds (Table 3).

Table 3. Comparison of the Lifetimes of S1 State Obtained from the Global Analysis of Transient Spectrum (τ_{TA}) and Fluorescence Lifetimes (τ_{F}) Obtained from Time-Resolved Emission Measurements in Acetonitrile or Benzonitrile

compound	τ_{TA} (ns)	τ_{F} (ns)
2a	5.23	5.23
2b	0.04	0.08
2c	4.53	4.69
3a	4.51	4.47
3b	0.04	0.12
3c	4.81	3.30

The data presented so far are in accordance to the expected photophysical behavior of **2a–2c** and **3a–3c**. For **2a** and **2c**, a very slow decay of the singlet excited state is observed on a nanosecond time scale. Similar lifetimes were observed by transient absorption and emission spectroscopy. However, for compound **2b**, a 100-fold increased decay rate of the S₁ state is observed. Similarly, for **3b**, a significantly increased decay rate of the S₁ state is observed, which is indicative of the occurrence of a substantially faster decay process. An explanation that is often invoked for such observations is the formation of a

charge-separated state that is stabilized in polar solvents. The proposed scheme for such a photophysical behavior is depicted in Figure 5.

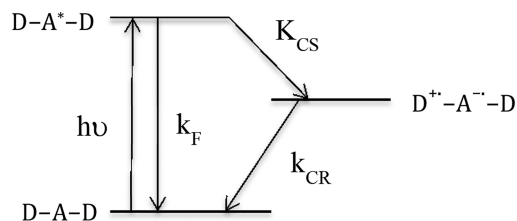


Figure 5. Schematic representation of photoinduced processes after photoillumination.

Although the initial excited state disappears, it is remarkable that we do not observe the characteristic absorption spectrum of the perylene radical anion of the CS state $\text{D}^+-\text{A}^--\text{D}$. For related compounds, CS states have been observed upon excitation,²⁷ but on some occasions spectroscopic evidence of charge separation is illusive.^{18,40} The absence of a CS absorption can be explained in a straightforward manner by assuming that charge recombination is faster than charge separation, which prevents accumulation of the CS state. For compounds **2b** and **3b** this implies that charge recombination rates are at least from 1×10^9 to $1 \times 10^{10} \text{ s}^{-1}$, respectively (Table S1).

Molecular Simulations. To gain more insight of the nature of the initial excited state in the studied compounds, we performed DFT calculations. The excitations of compounds **2a** and **2b** were calculated by TD-DFT using a DZP basis set consisting of Slater-type function and a M06-2X exchange-correlation function. All calculations were performed using the Amsterdam Density Functional theory package. The calculated absorption spectra of compounds **2a** and **2b** show a strong absorption feature with an oscillator strength close to 0.8 at 480 nm (Figure 6). In both cases, these absorptions mainly consist of the transition from highest occupied molecular orbital of

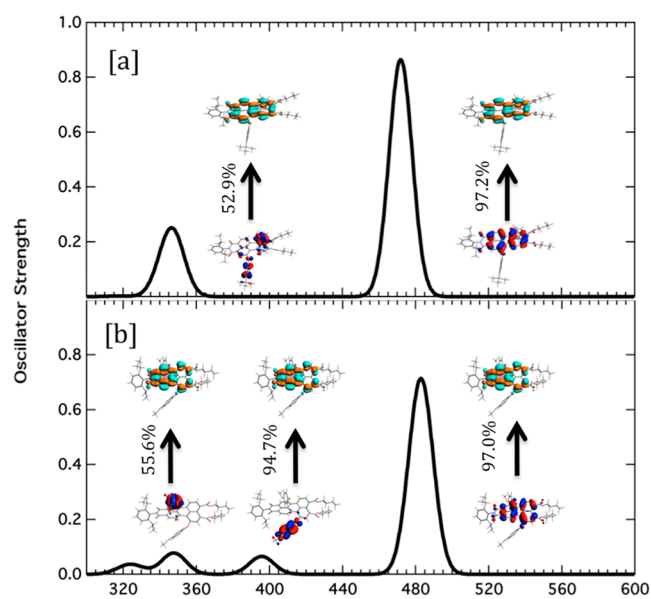


Figure 6. Optical excitation of **2a** (top) and **2b** (bottom) calculated using TD-DFT with DZP/M06-2X.

perylene (HOMO_{perylene}) to lowest unoccupied molecular orbital of perylene (LUMO_{perylene}). The computational transition energies are somewhat higher than those observed experimentally. This is attributed to the absence of solvent effects in the calculations that generally shift the absorption bands to lower energy.

In the calculated spectrum of **2a**, there is an additional absorption near 345 nm, which has transition from the HOMO of bay substituents to the LUMO of perylene core. For **2b**, multiple higher-lying bands are observed between 300 and 420 nm. All of these bands contain substantial contributions from the CT transitions from occupied orbitals of the substituents to the LUMO of the perylene core. These calculations show that for both compounds there is no clear low-energy CT state present in vacuum. However, note that the nature of the excited states is not necessarily the same in solution. First of all, the excited states with (partial) CT character will be stabilized considerably in highly polar solvents such as acetonitrile and benzonitrile and, therefore, arise much closer to the local excited state localized on the perylene core. From the calculations presented here, it can be seen that for **2b** the excited charge-separated states are lower in energy than for **2a**, which can be understood in terms of the stronger electron-donating character of the substituents in **2b**. Second, the presence of a polar solvent can also change the nature of the excited state considerably after excitation. This can result in the formation of a CT state that is not present in vacuum.

The results from the molecular simulations are in line with the experimental data obtained by TA and fluorescence spectroscopy. These experimental data reveal the formation of identical “locally excited states” for all compounds of the same class, irrespective of the electron-donating substituent attached. Subsequently, fluorescence takes place for compounds bearing weak donors in all solvents, while strong fluorescence quenching takes place for compounds bearing strong donors in polar solvents. The fluorescence quenching takes place by electron transfer from the electron donor to the perylene core. This process is thermodynamically favored and, from bay-attached electron donors, kinetically allowed. This charge-separation process occurs *after* the primary excitation process and is therefore not described by the molecular simulations based on DFT calculations.

CONCLUSIONS

We have synthesized a series of perylene tetracarboxylic acid derivatives, bearing electron-donating 4-methoxyphenoxy groups at 1,7-bay positions and, in two cases, also a 4-methoxyphenyl group at the imide position. Subsequent photophysical characterization of these compounds revealed the various variables that dictate the CT process in perylene-based systems; electronic nature of the perylene core, the position of electron donor, and the solvent polarity. For the perylene tetraester-based compound, which has the least electron-deficient perylene core, CT was observed only in polar acetonitrile. Upon moving to perylene monoimide diester, which has an increased electron deficiency due to presence of a more electron-withdrawing imide group, significant CT is observed already in chloroform. An efficient CT occurred in both polar and nonpolar solvents for the most electron-deficient perylene bisimide based compounds. From transient absorption spectroscopy and DFT calculations, it has been concluded that charge separation takes place after local excitation of the perylene core. The kinetics of CT is strongly

influenced by the positioning of the electron-donor on the perylene scaffold. Changing position from “bay” to “imide” exerted a significantly negative impact on the CT rates. In this way, this study has revealed that the photoinduced CT process can be precisely tuned in perylene-based systems by altering the electronic nature of the perylene core, the positioning of the electron donor, and the solvent polarity.

EXPERIMENTAL SECTION

Materials. All the reagents utilized in the synthesis were purchased from commercial suppliers, unless otherwise stated. The DMF used in the synthesis was of anhydrous grade. Toluene was dried over sodium under an argon atmosphere prior to use. All other solvents used in the syntheses were of reagent grade and were used as received from suppliers. The purifications of the products were performed by column chromatography (silica gel 60, mesh size 0.063–0.200 mm). For all the spectroscopic measurements, spectroscopy-grade solvents were purchased from commercial suppliers and were used as received.

Instrumentation and Characterization. The NMR spectra were recorded with 400 MHz pulsed Fourier transform NMR spectrometer in CDCl₃ at room temperature. The chemical shifts are quoted relative to tetramethylsilane (TMS). δ values are given in parts per million, and J values are in hertz. Electrochemical behavior of the compounds was studied by cyclic voltammetry in a three-electrode single-compartment cell consisting of a platinum sheet as the working electrode, Ag wire as the reference electrode, and a Pt wire as the counter electrode (scan rate = 0.5 V/s). Predried CH₂Cl₂ containing 0.1 M tetrabutylammonium hexafluorophosphate was used as solvent. The measurements were done under continuous flow of nitrogen. The concentration of the prepared samples was ca. 0.5 mM. Under these conditions, the ferrocene oxidation was observed at 0.52 V.

Absorption measurements were performed in PerkinElmer Lambda 40 UV–vis spectro-photometer. Photoluminescence studies were done in SPEX Fluorimeter. Fluorescence lifetimes were performed with LifeSpec-ps Fluorescence spectrometer with fixed excitation wavelength of 400 nm. For quantum yield measurements, the formula for optically dilute solutions was used.⁴² Fluorescence quantum yields of compounds **1–2** were determined by using perylene-3,4,9,10-tetracarboxylic tetrabutylester ($\phi_F = 0.98$ in CH₂Cl₂) as a reference, whereas, for compounds **3–4**, *N,N'*-bis(1-hexylheptyl)-perylene bisimide ($\phi_F = 0.99$ in CH₂Cl₂) was used.⁴³

Pump–probe transient-absorption measurements were performed by using tunable Yb:KGW laser system consisting of a YB:KGW laser (1028 nm), which operates at 5 kHz with a pulse duration of less than 180 fs (PHAROS-SP-06–200 Light Conversion) and an optical parametric amplifier (ORPHEUS-PO15F5HNP1, Light Conversion). A white light continuum probe pulse was generated by focusing part of the fundamental 1028 nm from Pharos into a sapphire crystal. Transient absorption data were collected using a commercial pump–probe spectrometer, HELIOS (Ultrafast Systems) in the wavelength range of 490–910 nm. The maximum time-delay between the pump and the probe pulse was 3.3 ns. The compounds were dissolved in spectroscopic grade toluene, chloroform, and acetonitrile/benzonitrile and placed in quartz cuvettes with a 2 mm path length. To prevent aggregation and photobleaching, the samples were stirred with a magnetic stirrer.

The geometrical and optical properties of the chromophores were investigated by DFT calculations using the Amsterdam Density Functional (ADF) software package. The geometry of the molecules was optimized using the PBE functional together with a double- ζ plus polarization (DZP) type basis set consisting of Slater functions. The optical absorption spectra were calculated by TD-DFT theory calculations using the M06-2X meta-GGA functional with a DZP basis set.

Synthesis of 1,7-Di(4-tert-butylphenoxy)perylene-3,4,9,10-tetracarboxy Tetrabutylester (1a). In a 25 mL round-bottomed flask, weighed amounts of 1,7-dibromoperylene tetrabutylester **1** (200 mg, 0.25 mmol), 4-tert-butylphenol (148 mg, 0.99 mmol), and Cs_2CO_3 (485 mg, 1.49 mmol) were taken. Subsequently, anhydrous DMF (8 mL) was added. The reaction mixture was stirred at 115 °C for 3 h under argon atmosphere. After the mixture cooled to room temperature, CH_2Cl_2 (50 mL) was added to the reaction mixture, and the resultant solution was washed with water several times. The organic layer was collected and evaporated. The crude product was chromatographed with dichloromethane (DCM) to afford the desired product **1a** (199 mg, 85%). Later, it was recrystallized from refluxing EtOH. ^1H NMR (400 MHz, CDCl_3): δ = 9.08 (d, J = 8.0 Hz, 2H), 7.98 (d, J = 8.0 Hz, 2H), 7.73 (s, 2H), 7.39 (d, J = 8.0 Hz, 4H), 7.01 (d, J = 8.0 Hz, 4H), 4.29 (t, J = 6.8 Hz, 4H), 4.23 (t, J = 6.8 Hz, 4H), 1.78–1.70 (m, 4H), 1.69–1.62 (m, 4H), 1.50–1.33 (m, 4H), 1.41–1.30 (m, 4H), 1.33 (s, 18H), 0.96 (t, J = 6.8 Hz, 6H), 0.89 ppm (t, J = 6.8 Hz, 6H). ^{13}C NMR (100 MHz, CDCl_3): δ = 168.5, 167.8, 153.3, 152.2, 147.0, 132.0, 131.2, 129.4, 129.1, 127.1, 127.0, 124.7, 124.3, 122.5, 118.3, 65.3, 65.2, 34.4, 31.4, 30.6, 30.4, 19.2, 19.1, 13.8, 13.7 ppm.

Synthesis of 1,7-Di(4-methoxyphenoxy)perylene-3,4,9,10-tetracarboxy Tetrabutylester (1b). Prepared from 1,7-dibromoperylene tetrabutylester **1** (100 mg, 0.12 mmol), 4-methoxyphenol (61 mg, 0.49 mmol), and Cs_2CO_3 (240 mg, 0.74 mmol) according to the procedure described for compound **1a**. The crude product was purified using silica-60/ CHCl_3 and, subsequently, recrystallized from refluxing ethanol (97 mg, 88%). ^1H NMR (400 MHz, CDCl_3): δ = 9.10 (d, J = 8.0 Hz, 2H), 7.99 (d, J = 8.0 Hz, 2H), 7.68 (s, 2H), 7.04 (d, J = 8.8 Hz, 4H), 6.92 (d, J = 8.8 Hz, 4H), 4.29 (t, J = 6.8 Hz, 4H), 4.23 (t, J = 6.8 Hz, 4H), 3.82 (s, 6H), 1.78–1.71 (m, 4H), 1.71–1.63 (m, 4H), 1.52–1.41 (m, 4H), 1.40–1.30 (m, 4H), 0.97 (t, J = 7.2 Hz, 6H), 0.90 ppm (t, J = 7.2 Hz, 6H). ^{13}C NMR (100 MHz, CDCl_3): δ = 168.5, 167.8, 156.4, 152.9, 149.0, 131.2, 131.1, 129.2, 129.0, 127.1, 124.4, 123.4, 121.8, 120.5, 115.2, 65.3, 65.2, 55.7, 30.6, 30.4, 19.2, 19.1, 13.8, 13.7 ppm.

Synthesis of N-(2,6-Diisopropylphenyl)-1,7-di(4-tert-butylphenoxy)perylene-3,4,9,10-tetracarboxy Monoimide Dibutylester (2a). A mixture of 4-tert-butylphenol (54 mg, 0.36 mmol), K_2CO_3 (100 mg, 0.72 mmol), and 18-Crown-6 (190 mg; 0.72 mmol) was stirred in anhydrous toluene (20 mL) for 20 min at room temperature under argon atmosphere. Subsequently, 1,7-dibromoperylene monoimide dibutylester **2** (100 mg, 0.12 mmol) was added, and the reaction mixture was stirred for 3 h at 95 °C. After the mixture cooled to room temperature, more toluene (30 mL) was added, and the organic solution was extracted with water twice. The solvent was evaporated, and the crude product was purified by silica gel column chromatography in DCM to afford compound **2a** (105 mg; 90%). ^1H NMR (400 MHz, CDCl_3): δ = 9.30 (t, J = 8.4 Hz, 2H), 8.61 (d, J = 8.4 Hz, 1H), 8.39 (s, 1H), 8.03 (d, J = 8.4

Hz, 1H), 7.78 (s, 1H), 7.46–7.38 (m, 5H), 7.29 (d, J = 8.0 Hz, 2H), 7.09–7.02 (m, 4H), 4.31 (t, J = 6.8 Hz, 2H), 4.24 (t, J = 6.8 Hz, 2H), 2.75–2.65 (m, 2H), 1.80–1.61 (m, 4H), 1.49–1.33 (m, 4H), 1.34 (s, 9H), 1.33 (s, 9H), 1.16–1.10 (m, 12H), 0.98 (t, J = 7.2 Hz, 3H), 0.91 ppm (t, J = 7.2 Hz, 3H). ^{13}C NMR (100 MHz, CDCl_3): δ = 168.4, 167.6, 163.7, 163.1, 153.9, 153.8, 153.1, 152.8, 147.6, 147.4, 145.6, 134.3, 132.6, 132.1, 130.8, 130.8, 130.70, 130.66, 129.4, 129.1, 128.4, 127.8, 127.2, 127.1, 125.8, 125.7, 125.2, 124.8, 123.9, 123.8, 122.8, 121.3, 121.1, 118.7, 118.3, 65.5, 65.4, 34.5, 34.4, 31.4, 30.6, 30.4, 29.1, 24.0, 23.9, 19.2, 19.1, 13.8, 13.7 ppm.

Synthesis of N-(2,6-Diisopropylphenyl)-1,7-di(4-methoxyphenoxy)perylene-3,4,9,10-tetracarboxy Monoimide Dibutylester (2b). Prepared from 4-methoxyphenol (40 mg, 0.32 mmol), K_2CO_3 (89 mg, 0.64 mmol), 18-Crown-6 (170 mg, 0.64 mmol), and 1,7-dibromoperylene monoimide dibutylester **2** (90 mg, 0.11 mmol) as per the procedure described for the compound **2a**. The crude product was purified by column chromatography (silica-60/ CHCl_3) and, subsequently, recrystallized from refluxing EtOH to afford the product **2b** (84 mg, 85%). ^1H NMR (400 MHz, CDCl_3): δ = 9.41 (t, J = 8.0 Hz, 2H), 8.64 (d, J = 8.0 Hz, 1H), 8.33 (s, 1H), 8.05 (d, J = 8.0 Hz, 1H), 7.73 (s, 1H), 7.45 (t, J = 7.6 Hz, 1H), 7.30 (d, J = 8.0 Hz, 2H), 7.09 (t, J = 8.8 Hz, 4H), 6.97 (d, J = 9.2 Hz, 2H), 6.94 (d, J = 9.2 Hz, 2H), 4.32 (t, J = 6.8 Hz, 2H), 4.25 (t, J = 6.8 Hz, 2H), 3.85 (s, 3H), 3.82 (s, 3H), 2.73–2.65 (m, 2H), 1.78–1.71 (m, 2H), 1.70–1.62 (m, 2H), 1.49–1.43 (m, 2H), 1.36–1.31 (m, 3H), 1.15–1.12 (m, 12H), 0.98 (t, J = 7.2 Hz, 3H), 0.91 ppm (t, J = 7.2 Hz, 3H). ^{13}C NMR (100 MHz, CDCl_3): δ = 167.9, 167.1, 163.1, 162.6, 156.3, 156.1, 154.1, 154.0, 148.3, 147.9, 145.1, 133.8, 132.0, 131.6, 130.3, 130.2, 130.13, 130.08, 128.91, 128.88, 128.5, 127.9, 127.3, 125.1, 124.6, 124.0, 123.8, 123.4, 122.3, 122.2, 120.5, 120.3, 119.9, 114.9, 114.9, 65.0, 64.9, 55.2, 30.1, 29.9, 28.6, 23.4, 18.7, 18.6, 13.3, 13.2 ppm.

Synthesis of N,N'-Bis(2,6-diisopropylphenyl)-1,7-di(4-tert-butylphenoxy)perylene-3,4,9,10-tetracarboxy Bisimide (3a). Prepared from 4-tert-butylphenol (53 mg, 0.35 mmol), K_2CO_3 (96 mg, 0.70 mmol), 18-Crown-6 (185 mg, 0.70 mmol), and 1,7-dibromoperylene bisimide **3** (100 mg, 0.12 mmol) in dry toluene (30 mL) at 90 °C according to the procedure described for compound **2a**. The crude product was refluxed in MeOH (20 mL) and filtered to remove unreacted phenol. Thereafter, the dried precipitate was chromatographed using silica-60/DCM to afford compound **3a** (91 mg, 79%). ^1H NMR (400 MHz, CDCl_3): δ = 9.67 (d, J = 8.0 Hz, 2H), 8.69 (d, J = 8.0 Hz, 2H), 8.45 (s, 2H), 7.46 (m, 6H), 7.32 (d, J = 7.2 Hz, 4H), 7.11 (d, J = 7.2 Hz, 4H), 2.72 (m, 4H), 1.36 (s, 18H), 1.20–1.12 ppm (m, 24H). ^{13}C NMR (100 MHz, CDCl_3): δ = 163.5, 162.9, 155.3, 152.6, 148.0, 145.6, 133.8, 130.7, 130.5, 129.7, 129.6, 129.0, 127.4, 125.8, 124.7, 124.5, 124.0, 122.3, 118.7, 31.4, 29.2, 24.0, 23.9 ppm.

Synthesis of N,N'-Bis(2,6-diisopropylphenyl)-1,7-di(4-methoxyphenoxy)perylene-3,4,9,10-tetracarboxy Bisimide (3b). Prepared from 4-methoxyphenol (86 mg, 0.69 mmol), K_2CO_3 (191 mg, 1.38 mmol), 18-Crown-6 (365 mg, 1.38 mmol), and 1,7-dibromoperylene bisimide **3** (200 mg, 0.23 mmol) in dry toluene (50 mL) according to the procedure described for compound **2a**. The crude product was refluxed in MeOH (25 mL) and filtered (after cooling) to remove unreacted phenol. Thereafter, the dried precipitate was chromatographed (silica-60/DCM/toluene 1:1) to afford compound **3b** (180 mg, 82%). ^1H NMR (400 MHz, CDCl_3):

δ = 9.71 (d, J = 8.0 Hz, 2H), 8.73 (d, J = 8.0 Hz, 2H), 8.41 (s, 2H), 7.48 (t, J = 7.6 Hz, 2H), 7.33 (d, J = 7.6 Hz, 4H), 7.16 (d, J = 7.6 Hz, 4H), 7.01 (d, J = 7.6 Hz, 4H), 3.85 (s, 6H), 2.74 (m, 4H), 1.17 ppm (s, 24H). ^{13}C NMR (100 MHz, CDCl_3): δ = 163.5, 162.9, 157.0, 156.0, 148.3, 145.6, 133.8, 130.6, 130.5, 129.6, 129.0, 125.6, 124.0, 123.9, 123.8, 122.2, 120.8, 115.6, 55.7, 29.2, 24.0 ppm.

Synthesis of *N*-(2,6-Diisopropylphenyl)-1,7-dibromoperylene-3,4,9,10-tetracarboxy Monoimide Monobenzimidazole (4 + 4'). 1,7-dibromo perylene monoimide monoanhydride **7** (50 mg, 0.07 mmol) and 1,2-diaminobenzene (10 mg, 0.09 mmol) were taken in propionic acid (10 mL). The mixture was refluxed for 3 h. After the mixture cooled to room temperature, it was poured into water to precipitate the crude product. The precipitate was filtered off and washed with several portions of water to remove all the propionic acid. The precipitate was dried and chromatographed on silica-60 eluting with DCM to afford the pure product (48 mg, 87%) as the mixture of two regioisomers **4** and **4'** in a ratio ca. 2:1. ^1H NMR (400 MHz, CDCl_3): δ = 9.60–9.50 (m, 2H), 9.22 (s, 0.35H), 9.11 (s, 0.65H), 8.99 (s, 1H), 8.94 (d, J = 8.0 Hz, 0.65H), 8.90 (d, J = 8.0 Hz, 0.35H), 8.78 (d, J = 8.0 Hz, 1H), 8.56–8.51 (m, 1H), 7.95–7.90 (m, 1H), 7.56–7.47 (m, 3H), 7.35 (d, J = 8.0 Hz, 2H), 2.79–2.70 (m, J = 6.8 Hz, 2H), 1.22–1.16 ppm (m, 12H). ^{13}C NMR spectra could not be measured because of its low solubility.

Synthesis of *N*-(2,6-Diisopropylphenyl)-1,7-di(4-*tert*-butylphenoxy)perylene-3,4,9,10-tetracarboxy Monoimide Monobenzimidazole (4a). Synthesized from 4-*tert*-butylphenol (59 mg, 0.39 mmol), K_2CO_3 (108 mg, 0.78 mmol), 18-Crown-6 (206 mg, 0.78 mmol), and 1,7-dibromoperylene monoimide monobenzimidazole **4** (100 mg, 0.13 mmol) in dry toluene (25 mL) according to the procedure described for compound **2a**. The crude product was chromatographed using silica-60/ CHCl_3 to afford compound **4a** (95 mg; 80%) as the mixture of two regioisomers. ^1H NMR (400 MHz, CDCl_3): δ = 9.68–9.52 (m, 2), 8.80–8.74 (m, 1H), 8.64–8.58 (m, 1.45 H), 8.52 (s, 0.55H), 8.49–8.45 (m, 0.60H), 8.42–8.36 (m, 1.50H), 7.83–7.75 (m, 1H), 7.51–7.38 (m, 7H), 7.30 (d, J = 7.6 Hz, 2H), 7.17–7.09 (m, 4H), 2.77–2.73 (m, 2H), 1.39–1.34 (m, 18H), 1.17–1.14 ppm (m, 12H). ^{13}C NMR spectrum could not be measured because of its low solubility.

Synthesis of *N*-(2,6-Diisopropylphenyl)-1,7-di(4-methoxyphenoxy)perylene-3,4,9,10-tetracarboxy Monoimide Monobenzimidazole (4b). Synthesized from 4-methoxyphenol (48 mg, 0.39 mmol), K_2CO_3 (108 mg, 0.78 mmol), 18-Crown-6 (206 mg, 0.78 mmol), and 1,7-dibromoperylene monoimide monobenzimidazole **4** (100 mg, 0.13 mmol) in dry toluene (30 mL) according to the procedure described for compound **2a**. The crude product was chromatographed using silica-60/ CHCl_3 to afford compound **4b** (96 mg, 86%) as the mixture of two regioisomers. ^1H NMR (400 MHz, CDCl_3): δ = 9.68–9.52 (m, 2H), 8.72 (d, J = 8.4 Hz, 1H), 8.65–8.55 (m, 1H), 8.50 (s, 0.55H), 8.41 (s, 0.45H), 8.40–8.29 (m, 2H), 7.77–7.71 (m, 1H), 7.46 (t, J = 8.0 Hz, 1H), 7.41–7.35 (m, 2H), 7.31 (d, J = 8.0 Hz, 2H), 7.22–7.13 (m, 4H), 7.08–6.94 (m, 4H), 3.89–3.83 (m, 6H), 2.77–2.73 (m, 2H), 1.19–1.13 ppm (m, 12H). ^{13}C NMR spectrum could not be measured because of its low solubility.

Synthesis of *N*-(4-Methoxyphenyl)-1,7-dibromoperylene-3,4,9,10-tetracarboxy Monoimide Dibutylester (6). A 25 mL round-bottomed flask was charged with 1,7-dibromoperylene monoanhydride dibutylester **5** (150 mg, 0.22 mmol), 4-

methoxyaniline (35 mg, 0.29 mmol), and propionic acid (6 mL). The reaction mixture was refluxed for 24 h. After it cooled to room temperature, the reaction mixture was poured into the water to precipitate the crude product. The precipitate was filtered off and washed with several portions of water to remove all the propionic acid. The precipitate was dried and chromatographed on silica, eluting with CH_2Cl_2 , to afford the desired product **6** (140 mg, 81%). ^1H NMR (400 MHz, CDCl_3): δ = 9.24 (d, J = 8.0 Hz, 1H), 9.21 (d, J = 8.0 Hz, 1H), 8.89 (s, 1H), 8.68 (d, J = 8.0 Hz, 1H), 8.34 (s, 1H), 8.13 (d, J = 8.0 Hz, 1H), 7.24 (d, J = 8.0 Hz, 2H), 7.08 (d, J = 8.0 Hz, 2H), 4.35 (t, J = 6.8 Hz, 4H), 3.88 (s, 3H), 1.84–1.75 (m, 4H), 1.53–1.46 (m, 4H), 1.00 ppm (t, J = 7.2 Hz, 6H). ^{13}C NMR (100 MHz, CDCl_3): δ = 167.7, 166.9, 166.8, 163.5, 162.95, 162.91, 159.7, 138.0, 136.8, 134.2, 133.7, 132.0, 131.9, 131.6, 130.8, 130.5, 130.4, 130.3, 129.6, 129.5, 129.1, 129.0, 128.2, 128.13, 128.11, 127.3, 127.0, 126.9, 122.2, 122.1, 120.3, 119.4, 114.8, 66.0, 65.8, 55.5, 30.6, 30.5, 19.3, 19.2, 19.1, 13.8, 13.7 ppm.

Synthesis of *N*-(4-Methoxyphenyl)-1,7-di(4-*tert*-butylphenoxy)perylene-3,4,9,10-tetracarboxy Monoimide Dibutylester (2c). Synthesized from 4-*tert*-butylphenol (50 mg, 0.33 mmol), K_2CO_3 (69 mg, 0.50 mmol), 18-Crown-6 (131 mg, 0.50 mmol), and 1,7-dibromoperylene monoimide dibutylester **6** (65 mg, 0.08 mmol) in dry toluene (12 mL) according to the procedure described for compound **2a**. The crude product was chromatographed using silica-60/DCM to afford compound **2c** (56 mg, 73%). ^1H NMR (400 MHz, CDCl_3): δ = 9.39 (d, J = 8.4 Hz, 2H), 8.58 (d, J = 8.4 Hz, 1H), 8.34 (s, 1H), 8.04 (d, J = 8.4 Hz, 1H), 7.77 (s, 1H), 7.45–7.38 (m, 4H), 7.20 (d, J = 8.8 Hz, 2H), 7.09–7.01 (m, 6H), 4.31 (t, J = 6.8 Hz, 2H), 4.24 (t, J = 6.8 Hz, 2H), 3.85 (s, 3H), 1.78–1.63 (m, 4H), 1.52–1.34 (m, 4H), 1.34 (s, 9H), 1.32 (s, 9H), 0.97 (t, J = 7.6 Hz, 3H), 0.90 ppm (t, J = 7.2 Hz, 3H). ^{13}C NMR (100 MHz, CDCl_3): δ = 168.3, 167.6, 163.9, 163.6, 159.5, 153.9, 153.0, 152.7, 147.7, 147.6, 134.3, 132.7, 132.0, 130.8, 130.7, 130.5, 129.5, 129.2, 129.0, 128.4, 127.7, 127.6, 127.2, 127.1, 125.3, 124.73, 124.70, 123.6, 122.7, 121.13, 121.10, 118.8, 118.7, 114.7, 77.3, 77.0, 76.7, 65.5, 65.4, 55.5, 34.5, 34.4, 31.4, 30.6, 30.4, 19.2, 19.1, 13.8, 13.7 ppm.

Synthesis of *N*-(2,6-Diisopropylphenyl)-*N'*-(4-methoxyphenyl)-1,7-dibromoperylene-3,4,9,10-tetracarboxy Bisimide (8). Synthesized as per the procedure described for compound **6** from 1,7-dibromoperylene monoimide monoanhydride **7** (150 mg, 0.21 mmol), 4-methoxyaniline (78 mg, 0.63 mmol), and propionic acid (8 mL). The reaction mixture was refluxed for 24 h. After it cooled to room temperature, the reaction mixture was poured into the water to precipitate the crude product. The precipitate was filtered off and washed with several portions of water to remove all the propionic acid. The precipitate was dried and chromatographed on silica, eluting with CH_2Cl_2 , to afford the desired product **8** (133 mg, 77%). ^1H NMR (400 MHz, CDCl_3): δ = 9.56 (d, J = 8.0 Hz, 1H), 9.54 (d, J = 8.0 Hz, 1H), 9.00 (s, 1H), 8.98 (s, 1H), 8.79 (d, J = 8.0 Hz, 1H), 8.77 (d, J = 8.0 Hz, 1H), 7.51 (t, J = 7.6 Hz, 1H), 7.35 (d, J = 7.6 Hz, 2H), 7.24 (d, J = 8.8 Hz, 2H), 7.09 (d, J = 8.8 Hz, 2H), 3.89 (s, 3H), 2.78–2.66 (m, 2H), 1.19 (s, 6H), 1.17 ppm (s, 6H). ^{13}C NMR (100 MHz, CDCl_3): δ = 162.7, 162.5, 159.8, 145.6, 138.4, 138.3, 133.2, 133.1, 131.0, 130.6, 130.4, 130.1, 129.9, 129.6, 129.5, 129.4, 129.0, 128.7, 127.6, 127.4, 127.1, 124.2, 123.4, 123.0, 122.8, 120.9, 114.9, 55.5, 29.3, 23.99, 23.97 ppm.

Synthesis of N-(2,6-Diisopropylphenyl)-N'-(4-methoxyphenyl)-1,7-di(4-tert-butylphenoxy)perylene-3,4,9,10-tetracarboxy Bisimide (3c). Synthesized as per the procedure described for compound 2a from 4-tert-butylphenol (50 mg, 0.33 mmol), K₂CO₃ (69 mg, 0.50 mmol), 18-Crown-6 (131 mg, 0.50 mmol), and 1,7-dibromoperylene bisimide 8 (65 mg, 0.08 mmol) in dry toluene (12 mL) according to the procedure described for compound 2a. The crude product was chromatographed using silica-60/DCM to afford compound 2c (65 mg, 85%). ¹H NMR (400 MHz, CDCl₃): δ = 9.67 (d, J = 8.0 Hz, 1H), 9.62 (d, J = 8.0 Hz, 1H), 8.70 (d, J = 8.0 Hz, 1H), 8.62 (d, J = 8.0 Hz, 1H), 8.43 (s, 1H), 8.35 (s, 1H), 7.50–7.42 (m, 5H), 7.31 (d, J = 8.0 Hz, 2H), 7.22 (d, J = 8.8 Hz, 2H), 7.15–7.01 (m, 6H), 3.86 (s, 3H), 2.77–2.67 (m, 2H), 1.35 (s, 9H), 1.34 (s, 9H), 1.25–1.11 ppm (m, 12H). ¹³C NMR (100 MHz, CDCl₃): δ = 163.5, 163.3, 159.6, 155.5, 155.4, 152.5, 152.4, 148.2, 148.1, 145.6, 133.8, 133.7, 130.7, 130.5, 130.4, 129.6, 129.5, 129.4, 129.0, 128.9, 127.4, 127.3, 125.7, 125.3, 124.4, 124.24, 124.20, 124.0, 123.8, 122.3, 122.2, 119.0, 118.9, 114.7, 55.5, 36.8, 34.6, 34.5, 31.4, 29.2, 24.0, 23.9 ppm.

■ ASSOCIATED CONTENT

● Supporting Information

The Supporting Information is available free of charge on the ACS Publications website at DOI: 10.1021/acs.jpca.7b03806.

Calculated rate of fluorescence and fluorescence quenching; absorption and emission spectra of compounds 1–4a in chloroform; absorption and emission spectra of compounds 2c and 3c in chloroform; fluorescence decay curves of compounds 1a–b and 2a–c; fluorescence decay curves of compounds 3a–c and 4a–b; transient absorption spectra of compounds 2a–c and 3a–c; ¹H and ¹³C NMR spectra of all synthesized compounds (PDF)

■ AUTHOR INFORMATION

Corresponding Authors

*E-mail: W.F.Jager@tudelft.nl. (W.F.J.)

*E-mail: F.C.Grozema@tudelft.nl. (F.C.G.)

Notes

The authors declare no competing financial interest.

■ ACKNOWLEDGMENTS

Financial support from the Foundation for Fundamental Research on Matter, which is part of The Netherlands Organization for Scientific Research, is gratefully acknowledged. This research has also received funding from the European Research Council Horizon 2020 ERC Grant No. 648433.

■ REFERENCES

- (1) Alstrum-Acevedo, J. H.; Brennaman, M. K.; Meyer, T. J. Chemical Approaches to Artificial Photosynthesis. 2. *Inorg. Chem.* **2005**, *44* (20), 6802–6827.
- (2) Gust, D.; Moore, T. A.; Moore, A. L. Solar Fuels via Artificial Photosynthesis. *Acc. Chem. Res.* **2009**, *42* (12), 1890–1898.
- (3) Frischmann, P. D.; Mahata, K.; Würthner, F. Powering the future of molecular artificial photosynthesis with light-harvesting metallosupramolecular dye assemblies. *Chem. Soc. Rev.* **2013**, *42* (4), 1847–1870.
- (4) Wasielewski, M. R. Photoinduced electron transfer in supramolecular systems for artificial photosynthesis. *Chem. Rev.* **1992**, *92* (3), 435–461.
- (5) Gust, D.; Moore, T. A.; Moore, A. L. Molecular mimicry of photosynthetic energy and electron transfer. *Acc. Chem. Res.* **1993**, *26* (4), 198–205.
- (6) Paddon-Row, M. N. Investigating long-range electron-transfer processes with rigid, covalently linked donor-(norbornylogous bridge)-acceptor systems. *Acc. Chem. Res.* **1994**, *27* (1), 18–25.
- (7) Lewis, F. D.; Letsinger, R. L.; Wasielewski, M. R. Dynamics of Photoinduced Charge Transfer and Hole Transport in Synthetic DNA Hairpins. *Acc. Chem. Res.* **2001**, *34* (2), 159–170.
- (8) Wenger, O. S. How Donor–Bridge–Acceptor Energetics Influence Electron Tunneling Dynamics and Their Distance Dependences. *Acc. Chem. Res.* **2011**, *44* (1), 25–35.
- (9) Guldi, D. M.; Hirsch, A.; Scheloske, M.; Dietel, E.; Troisi, A.; Zerbetto, F.; Prato, M. Modulating Charge-Transfer Interactions in Topologically Different Porphyrin–C60 Dyads. *Chem. - Eur. J.* **2003**, *9* (20), 4968–4979.
- (10) Dubey, R. K.; Inan, D.; Sengupta, S.; Sudholter, E. J. R.; Grozema, F. C.; Jager, W. F. Tunable and highly efficient light-harvesting antenna systems based on 1,7-perylene-3,4,9,10-tetracarboxylic acid derivatives. *Chemical Science* **2016**, *7* (6), 3517–3532.
- (11) Wasielewski, M. R. Self-Assembly Strategies for Integrating Light Harvesting and Charge Separation in Artificial Photosynthetic Systems. *Acc. Chem. Res.* **2009**, *42* (12), 1910–1921.
- (12) Youngblood, W. J.; Lee, S.-H. A.; Maeda, K.; Mallouk, T. E. Visible Light Water Splitting Using Dye-Sensitized Oxide Semiconductors. *Acc. Chem. Res.* **2009**, *42* (12), 1966–1973.
- (13) Kärkäs, M. D.; Verho, O.; Johnston, E. V.; Åkermark, B. Artificial Photosynthesis: Molecular Systems for Catalytic Water Oxidation. *Chem. Rev.* **2014**, *114* (24), 11863–12001.
- (14) Würthner, F. Perylene bisimide dyes as versatile building blocks for functional supramolecular architectures. *Chem. Commun.* **2004**, *14*, 1564–1579.
- (15) Huang, C.; Barlow, S.; Marder, S. R. Perylene-3,4,9,10-tetracarboxylic Acid Diimides: Synthesis, Physical Properties, and Use in Organic Electronics. *J. Org. Chem.* **2011**, *76* (8), 2386–2407.
- (16) Langhals, H.; Saulich, S. Bichromophoric Perylene Derivatives: Energy Transfer from Non-Fluorescent Chromophores. *Chem. - Eur. J.* **2002**, *8* (24), 5630–5643.
- (17) Hippus, C.; Schlosser, F.; Vysotsky, M. O.; Böhmer, V.; Würthner, F. Energy Transfer in Calixarene-Based Cofacial-Positioned Perylene Bisimide Arrays. *J. Am. Chem. Soc.* **2006**, *128* (12), 3870–3871.
- (18) Flamigni, L.; Ventura, B.; You, C.-C.; Hippus, C.; Würthner, F. Photophysical Characterization of a Light-Harvesting Tetra Naphthalene Imide/Perylene Bisimide Array. *J. Phys. Chem. C* **2007**, *111* (2), 622–630.
- (19) Dubey, R. K.; Niemi, M.; Kaunisto, K.; Stranius, K.; Efimov, A.; Tkachenko, N. V.; Lemmetyinen, H. Excited-State Interaction of Red and Green Perylene Diimides with Luminescent Ru(II) Polypyridine Complex. *Inorg. Chem.* **2013**, *52* (17), 9761–9773.
- (20) Blas-Ferrando, V. M.; Ortiz, J.; Ohkubo, K.; Fukuzumi, S.; Fernandez-Lazaro, F.; Sastre-Santos, A. Submillisecond-lived photoinduced charge separation in a fully conjugated phthalocyanine-perylenebenzimidazole dyad. *Chemical Science* **2014**, *5* (12), 4785–4793.
- (21) Wasielewski, M. R. Energy, Charge, and Spin Transport in Molecules and Self-Assembled Nanostructures Inspired by Photosynthesis. *J. Org. Chem.* **2006**, *71* (14), 5051–5066.
- (22) Dubey, R. K.; Niemi, M.; Kaunisto, K.; Efimov, A.; Tkachenko, N. V.; Lemmetyinen, H. Direct Evidence of Significantly Different Chemical Behavior and Excited-State Dynamics of 1,7- and 1,6-Regioisomers of Pyrrolidinyl-Substituted Perylene Diimide. *Chem. - Eur. J.* **2013**, *19* (21), 6791–6806.
- (23) Shibano, Y.; Umeyama, T.; Matano, Y.; Tkachenko, N. V.; Lemmetyinen, H.; Araki, Y.; Ito, O.; Imahori, H. Large Reorganization Energy of Pyrrolidine-Substituted Perylenediimide in Electron Transfer. *J. Phys. Chem. C* **2007**, *111* (16), 6133–6142.
- (24) Gorczak, N.; Renaud, N.; Tarkuc, S.; Houtepen, A. J.; Eelkema, R.; Siebbeles, L. D. A.; Grozema, F. C. Charge transfer versus

molecular conductance: molecular orbital symmetry turns quantum interference rules upside down. *Chemical Science* **2015**, *6* (7), 4196–4206.

(25) Shoer, L. E.; Eaton, S. W.; Margulies, E. A.; Wasielewski, M. R. Photoinduced Electron Transfer in 2,5,8,11-Tetrakis-Donor-Substituted Perylene-3,4:9,10-bis(dicarboximides). *J. Phys. Chem. B* **2015**, *119* (24), 7635–7643.

(26) Pagoaga, B.; Mongin, O.; Caselli, M.; Vanossi, D.; Momicchioli, F.; Blanchard-Desce, M.; Lemercier, G.; Hoffmann, N.; Ponterini, G. Optical and photophysical properties of anisole- and cyanobenzene-substituted perylene diimides. *Phys. Chem. Chem. Phys.* **2016**, *18* (6), 4924–4941.

(27) Flamigni, L.; Ventura, B.; Barbieri, A.; Langhals, H.; Wetzel, F.; Fuchs, K.; Walter, A. On/Off Switching of Perylene Tetracarboxylic Bisimide Luminescence by Means of Substitution at the N-Position by Electron-Rich Mono-, Di-, and Trimethoxybenzenes. *Chem. - Eur. J.* **2010**, *16* (45), 13406–13416.

(28) Sengupta, S.; Dubey, R. K.; Hoek, R. W. M.; van Eeden, S. P. P.; Gunbaş, D. D.; Grozema, F. C.; Sudhölter, E. J. R.; Jäger, W. F. Synthesis of Regioisomerically Pure 1,7-Dibromoperylene-3,4,9,10-tetracarboxylic Acid Derivatives. *J. Org. Chem.* **2014**, *79* (14), 6655–6662.

(29) Dubey, R. K.; Efimov, A.; Lemmetyinen, H. 1,7- And 1,6-Regioisomers of Diphenoxy and Dipyrroliidyl Substituted Perylene Diimides: Synthesis, Separation, Characterization, and Comparison of Electrochemical and Optical Properties. *Chem. Mater.* **2011**, *23* (3), 778–788.

(30) Yuan, Z.; Xiao, Y.; Li, Z.; Qian, X. Efficient Synthesis of Regioisomerically Pure Bis(trifluoromethyl)-Substituted 3,4,9,10-Perylene Tetracarboxylic Bis(benzimidazole). *Org. Lett.* **2009**, *11* (13), 2808–2811.

(31) Perrin, L.; Hudhomme, P. Synthesis, Electrochemical and Optical Absorption Properties of New Perylene-3,4:9,10-bis-(dicarboximide) and Perylene-3,4:9,10-bis(benzimidazole) Derivatives. *Eur. J. Org. Chem.* **2011**, *2011* (28), 5427–5440.

(32) Dubey, R. K.; Westerveld, N.; Sudholter, E. J. R.; Grozema, F. C.; Jäger, W. F. Novel derivatives of 1,6,7,12-tetrachloroperylene-3,4,9,10-tetracarboxylic acid: synthesis, electrochemical and optical properties. *Org. Chem. Front.* **2016**, *3* (11), 1481–1492.

(33) Xue, C.; Sun, R.; Annab, R.; Abadi, D.; Jin, S. Perylene monoanhydride diester: a versatile intermediate for the synthesis of unsymmetrically substituted perylene tetracarboxylic derivatives. *Tetrahedron Lett.* **2009**, *50* (8), 853–856.

(34) Würthner, F.; Saha-Möller, C. R.; Fimmel, B.; Ogi, S.; Leowanawat, P.; Schmidt, D. Perylene Bisimide Dye Assemblies as Archetype Functional Supramolecular Materials. *Chem. Rev.* **2016**, *116* (3), 962–1052.

(35) Echue, G.; Lloyd-Jones, G. C.; Faul, C. F. J. Chiral Perylene Diimides: Building Blocks for Ionic Self-Assembly. *Chem. - Eur. J.* **2015**, *21* (13), 5118–5128.

(36) Würthner, F.; Thalacker, C.; Diele, S.; Tschierske, C. Fluorescent J-type Aggregates and Thermotropic Columnar Mesophases of Perylene Bisimide Dyes. *Chem. - Eur. J.* **2001**, *7* (10), 2245–2253.

(37) Vajiravelu, S.; Ramunas, L.; Juozas Vidas, G.; Valentas, G.; Vygintas, J.; Valiyaveetil, S. Effect of substituents on the electron transport properties of bay substituted perylene diimide derivatives. *J. Mater. Chem.* **2009**, *19* (24), 4268–4275.

(38) Escudero, D. Revising Intramolecular Photoinduced Electron Transfer (PET) from First-Principles. *Acc. Chem. Res.* **2016**, *49* (9), 1816–1824.

(39) Zweig, A.; Hodgson, W. G.; Jura, W. H. The Oxidation of Methoxybenzenes. *J. Am. Chem. Soc.* **1964**, *86* (19), 4124–4129.

(40) Dubey, R. K.; Knorr, G.; Westerveld, N.; Jäger, W. F. Fluorescent PET probes based on perylene-3,4,9,10-tetracarboxylic tetraesters. *Org. Biomol. Chem.* **2016**, *14* (5), 1564–1568.

(41) Fron, E.; Pilot, R.; Schweitzer, G.; Qu, J.; Herrmann, A.; Mullen, K.; Hofkens, J.; Van der Auweraer, M.; De Schryver, F. C. Photoinduced electron-transfer in perylenediimide triphenylamine-

based dendrimers: single photon timing and femtosecond transient absorption spectroscopy. *Photochemical & Photobiological Sciences* **2008**, *7* (5), 597–604.

(42) Crosby, G. A.; Demas, J. N. Measurement of photoluminescence quantum yields. Review. *J. Phys. Chem.* **1971**, *75* (8), 991–1024.

(43) Langhals, H.; Karolin, J.; Johansson, L. B.-A. Spectroscopic properties of new and convenient standards for measuring fluorescence quantum yields. *J. Chem. Soc., Faraday Trans.* **1998**, *94* (19), 2919–2922.